

# Fast-Forward Assisted STIRAP

Shumpei Masuda<sup>1, a)</sup> and Stuart A. Rice<sup>1, b)</sup>

*James Franck Institute, The University of Chicago, Chicago,  
IL 60637*

(Dated: 3 March 2022)

We consider combined stimulated Raman adiabatic passage (STIRAP) and fast-forward field (FFF) control of selective vibrational population transfer in a polyatomic molecule. The motivation for using this combination control scheme is twofold: (i) to overcome transfer inefficiency that occurs when the STIRAP fields and pulse durations must be restricted to avoid excitation of population transfers that compete with the targeted transfer and (ii) to overcome transfer inefficiency resulting from embedding of the actively driven subset of states in a large manifold of states. We show that, in a subset of states that is coupled to background states, a combination of STIRAP and FFFs that do not individually generate processes that are competitive with the desired population transfer can generate greater population transfer efficiency than can ordinary STIRAP with similar field strength and/or pulse duration. The vehicle for our considerations is enhancing the yield of HNC in the driven ground state-to-ground state nonrotating  $\text{HCN} \rightarrow \text{HNC}$  isomerization reaction and selective population of one of a pair of near degenerate states in nonrotating  $\text{SCCl}_2$ .

## I. INTRODUCTION

It is now well established that it is possible to actively control the quantum dynamics of a system by manipulating the frequency, phase and temporal character of an applied optical field<sup>1,2</sup>. The underlying mechanisms of all the proposed and experimentally demonstrated active control methods

rely on coherence and interference effects embedded in the quantum dynamics. Although the various control protocols provide prescriptions for the calculation of the control field, in general, the manifold of states of the driven system is too complicated to permit exact calculation of that field. That difficulty has led to the consideration of control of the quantum dynamics with a simplified Hamiltonian, e.g. within a subset of states without regard for the influence of the remaining background states. One exam-

---

<sup>a)</sup>Department of Physics, Tohoku University, Sendai 980, Japan; Electronic mail: masuda@uchicago.edu

<sup>b)</sup>Electronic mail: s-rice@uchicago.edu

ple of this class of control methods is the use of stimulated Raman adiabatic passage (STIRAP)<sup>3-7</sup> to transfer population within a three state subset of a larger manifold of states. Various extended STIRAP methods, involving more than three states, also have been proposed<sup>8-13</sup>. This simplification is not always acceptable: when the transition dipole moments between a selected subset of states and the other (background) states of the manifold are not negligible it is necessary to account for the influence of transitions involving the background states on the efficiency of the population transfer. Furthermore, STIRAP relies on adiabatic driving in which the populations in the instantaneous eigenstates of the Hamiltonian are constant. Because an adiabatic process must be carried out very slowly, at a rate much smaller than the frequencies of transitions between states of the Hamiltonian, the field strength and/or pulse duration imposed must be restricted to avert unwanted processes. Recognition of this restriction has led to the development of control protocols which we call assisted adiabatic transformations; these transformations typically use an auxiliary field to produce, with overall weaker driving fields and/or in a shorter time, and without excitation of competing processes, the desired target state population.

In an early study of a version of assisted

adiabatic population transfer, Kurkal and Rice<sup>11</sup> used the extended STIRAP process devised by Kobrak and Rice<sup>8</sup> to study vibrational energy transfer between an initial state and two nearly degenerate states in nonrotating  $\text{SCCl}_2$ . The extended STIRAP process, which is designed to control the ratio of the populations transferred to the target states, uses three pulsed fields: a pump field, a Stokes field, and a field that couples the target state to a so-called branch state. The ratio of populations of the target states that can be achieved depends on, and is limited by, the ratio of the dipole transition moments between the branch state and the target states, and is discretely controllable by suitable choice of the branch state from the manifold of states. Because the extended STIRAP process exploits adiabatic population transfer, the field strengths and pulse durations used must satisfy the same constraints as for a simple adiabatic population transfer.

Other assisted adiabatic transformation control methods include the counter-diabatic protocol<sup>14-17</sup>, the invariant-based inverse engineering protocol<sup>18</sup> and the fast-forward protocol<sup>19-23</sup>.

We have shown elsewhere<sup>24</sup> that, in a subset of states that is coupled to background states, a combination of STIRAP fields and a counter-diabatic field (CDF) can generate

greater population transfer efficiency than can ordinary STIRAP with necessarily restricted field strength and/or pulse duration. And it has been shown that the exact CDF for an isolated three level system is a useful approximation to the CDF for three and five state sub-manifolds embedded in a large manifold of states.

In this paper we complement our previous study with an examination of the use of combined phase-controlled STIRAP and fast-forward fields (FFFs) to control selective vibrational population transfer in a polyatomic molecule under conditions that require restriction of the STIRAP field strength and/or pulse duration. Again using selective vibrational energy transfer to drive the rotationless  $\text{HCN} \rightarrow \text{HNC}$  isomerization reaction and state-to-state vibrational energy transfer in an isolated nonrotating  $\text{SCCl}_2$  molecule as vehicles for our study it is shown that the phase-controlled STIRAP + FFF that affects complete transfer of population in an isolated three-level system is a useful approximation to the control field that affects efficient transfer of population for a three-state system embedded in background states. The FFF suppresses the influence of background states strongly coupled to the STIRAP pumped subset of states.

## II. FAST-FORWARD ASSISTED STIRAP

The fast-forward protocol is constructed to control the rate of evolution of particles between selected initial and target states in a continuous system. It can be regarded as defining a trajectory in the state space connecting the initial and final states for which the control field that accelerates the initial-to-final state transition is realizable. The time-dependent intermediate states acquire, relative to the states along the original trajectory of the initial-to-final state transition without the FFF acceleration<sup>19</sup> or the adiabatic transition<sup>20</sup>, an additional time-dependent phase. The fast-forward protocol has been extended to treat spatially discrete systems, e.g. accelerated manipulation of a Bose-Einstein condensate (BEC) in an optical lattice by Masuda and Rice<sup>23</sup>, and spin systems<sup>25</sup>, and a variant of this method can be used to accelerate selective population transfer between states in a discrete spectrum of states of a molecule.

### A. Fast-Forward Protocol for Discrete Systems

We consider a manifold of discrete states  $\{|i\rangle\}$  and time dependent transition (hopping) rates  $\omega_{l,m}$  between states  $|l\rangle, |m\rangle \in$

$\{|i\rangle\}$ . Note that these transition rates depend on the applied field and are the analogues of the Stokes and Raman frequencies in a STIRAP process; they are not the conventional transition probabilities. The derivation of the fast-forward driving fields proceeds in the same manner as described in Ref. 23. The equation of motion of the system wave function takes the form

$$i\frac{d\Psi(m,t)}{dt} = \sum_l \omega_{m,l}(R(t))\Psi(l,t) + \frac{V_0(m, R(t))}{\hbar}\Psi(m,t), \quad (1)$$

where  $\Psi(m,t)$  is the coefficient of  $|m\rangle$  and  $R$  is a time-dependent parameter characterizing the temporal dependence of  $\omega_{m,l}$ . Eq. (1) describes the population transfer among molecular states with  $\omega_{m,l}$  corresponding to the Rabi frequency of the laser field coupling the states  $|l\rangle$  and  $|m\rangle$  and  $V_0(m)$  the energy of the field-free state  $|m\rangle$ . Hereafter we refer to  $V_0(m)$  as a potential. Now let  $\phi_n(m, R)$  and  $E_n(R)$  be the wave function (coefficient of  $|m\rangle$ ) and energy of the  $n$ th eigenstate of the instantaneous Hamiltonian; they satisfy the time-independent discrete Schrödinger equation

$$\sum_l \hbar\omega_{m,l}(R)\phi_n(l, R) + V_0(m, R)\phi_n(m, R) = E_n(R)\phi_n(m, R). \quad (2)$$

We seek the transition rates and potential that generates

$\phi_n(m, R_f) \exp[-(i/\hbar) \int_0^{T_F} E_n(R(t'))dt']$  from  $\phi_n(m, R_i)$ , where  $R(T_F) = R_f$ . Although such dynamics is realized as a solution of Eq. (1) if  $dR(t)/dt$  is sufficiently small, corresponding to an adiabatic process, if  $dR(t)/dt$  is not very small unwanted excitations occur. We consider a time-dependent intermediate state wave function  $\Psi_{\text{FF}}$  that evolves from  $\phi_n(m, R_i)$  to  $\phi_n(m, R_f) \exp[-(i/\hbar) \int_0^{T_F} E_n(R(t'))dt']$  in time  $T_F$ . The Schrödinger equation for  $\Psi_{\text{FF}}$  is

$$i\frac{d\Psi_{\text{FF}}(m,t)}{dt} = \sum_l \omega_{m,l}^{\text{FF}}(t)\Psi_{\text{FF}}(l,t) + \frac{V_{\text{FF}}(m,t)}{\hbar}\Psi_{\text{FF}}(m,t), \quad (3)$$

and the transition rates  $\omega_{m,l}^{\text{FF}}$  between  $|l\rangle$  and  $|m\rangle$  are time-dependent and/or tunable. The wave function  $\Psi_{\text{FF}}(m,t)$  is assumed to be represented, with the additional phase  $f(m,t)$ , in the form

$$\Psi_{\text{FF}}(m,t) = \phi_n(m, R(t)) \exp[i f(m,t)] \times \exp\left[-\frac{i}{\hbar} \int_0^t E_n(R(t'))dt'\right]. \quad (4)$$

We require that  $f(m, 0) = f(m, T_F) = 0$ . Assuming  $\Psi_{\text{FF}}(m,t) \neq 0$  ( $\phi_n(m, R(t)) \neq 0$ ) we divide Eq. (3) by  $\Psi_{\text{FF}}(m,t)$ , substitute into Eq. (4), and then decompose the equation into real and imaginary parts. The imagi-

nary part of the equation leads to

$$\begin{aligned} & \frac{dR}{dt} \text{Re} \left[ \phi_n^*(m, R) \frac{\partial \phi_n(m, R)}{\partial R} \right] \\ &= \sum_l \text{Im} \left[ \phi_n^*(m, R) \phi_n(l, R) \right. \\ & \times \left( \omega_{m,l}^{\text{FF}}(t) \exp [i(f(l, t) - f(m, t))] \right. \\ & \left. \left. - \omega_{m,l}(R(t)) \right) \right] \end{aligned} \quad (5)$$

and the real part leads to the driving potential

$$\begin{aligned} V_{\text{FF}}(m, t) &= V_0(m, R(t)) \\ &+ \sum_l \text{Re} \left[ \hbar \frac{\phi_n(l, R(t))}{\phi_n(m, R(t))} \left( \omega_{m,l}(R(t)) - \omega_{m,l}^{\text{FF}}(t) \right) \right. \\ & \times \exp [i(f(l, t) - f(m, t))] \left. \right] - \hbar \frac{df(m, t)}{dt} \\ &- \hbar \frac{dR}{dt} \text{Im} \left[ \frac{1}{\phi_n(m, R(t))} \frac{\partial \phi_n(m, R(t))}{\partial R} \right]. \end{aligned} \quad (6)$$

When  $\phi_n(m, R) = 0$  for any  $R$ , the Schrödinger equation (3) takes the form

$$\sum_l \omega_{m,l}^{\text{FF}}(t) e^{ifl} \phi_n(l, R(t)) = 0, \quad (7)$$

and Eq. (2) becomes

$$\sum_l \omega_{m,l}(R(t)) \phi_n(l, R(t)) = 0. \quad (8)$$

If  $\phi_n(m, R(t)) = 0$  for any  $t$  the driving potential is arbitrary because it has no influence in the Schrödinger equation.

## B. Application to a STIRAP Process

In its simplest form STIRAP is used to transfer population between states  $|1\rangle$  and  $|3\rangle$  in a three state manifold in which transitions  $|1\rangle \rightarrow |2\rangle$  and  $|2\rangle \rightarrow |3\rangle$  are allowed but

$|1\rangle \rightarrow |3\rangle$  is forbidden. The driving optical field consists of two suitably timed and overlapping laser pulses with the (Stokes) pulse driving the  $|2\rangle \rightarrow |3\rangle$  transition preceding the (pump) pulse driving the  $|1\rangle \rightarrow |2\rangle$  transition. The field dressed states of this system are combinations of the bare states  $|1\rangle$  and  $|3\rangle$  with coefficients that depend on the Rabi frequencies of the pump ( $\Omega_p$ ) and Stokes ( $\Omega_S$ ) fields. Consequently, as those fields vary in time there is an adiabatic transfer of population from  $|1\rangle$  to  $|3\rangle$ . In the three-state system the efficiency of STIRAP is relatively insensitive to the details of the pulse profile and the pulse separation<sup>6</sup> when the adiabatic condition  $\Delta T(\Omega_S^2 + \Omega_p^2)^{1/2} > 10$  can be met, where  $\Delta T$  is the pulse overlap. Using the interaction representation and the rotating wave approximation (RWA), the Hamiltonian of the three-state system with resonant pump  $|1\rangle \rightarrow |2\rangle$  and Stokes  $|2\rangle \rightarrow |3\rangle$  fields can be represented in the form

$$H_{\text{RWA}}(t) = -\hbar \begin{pmatrix} 0 & \Omega_p(t) & 0 \\ \Omega_p(t) & 0 & \Omega_S(t) \\ 0 & \Omega_S(t) & 0 \end{pmatrix} \quad (9)$$

with  $\Omega_p$  and  $\Omega_S$  the Rabi frequencies defined by

$$\begin{aligned} \Omega_p(t) &= \mu_{12} E_p^{(e)}(t)/(2\hbar), \\ \Omega_S(t) &= \mu_{23} E_S^{(e)}(t)/(2\hbar), \end{aligned} \quad (10)$$

where  $E_{p(S)}^{(e)}$  is the envelope of the amplitude of the pump (Stokes) field and  $\mu_{ij}$  the transi-

tion dipole moment between states  $|i\rangle$  and  $|j\rangle$ . Note that, by assumption,  $\mu_{13} = 0$ . The time-dependent field-dressed eigenstates of this system are linear combinations of the field-free states with coefficients that depend on the Stokes and pump field magnitudes and the transition dipole moments. The field-dressed state of interest to us is

$$|\phi_2(t)\rangle = \cos \Theta(t)|1\rangle - \sin \Theta(t)|3\rangle, \quad (11)$$

where

$$\tan \Theta(t) = \frac{\Omega_p(t)}{\Omega_S(t)}. \quad (12)$$

Because the Stokes pulse is applied before but overlaps the pump pulse, initially  $\Omega_p \ll \Omega_S$  and all of the population is initially in field-free state  $|1\rangle$ . At the final time  $\Omega_p \gg \Omega_S$  so all of the population in  $|\phi_2(t)\rangle$  projects onto the target state  $|3\rangle$ . Note that  $|\phi_2(t)\rangle$  has no projection on the intermediate field-free state  $|2\rangle$ . Suppose now that either the pulsed field duration or the field strength must be restricted to avoid exciting unwanted processes that compete with the desired population transfer, with the consequence that the condition  $\Delta T(\Omega_S^2 + \Omega_p^2)^{1/2} > 10$  cannot be met. Then the STIRAP process generates incomplete population transfer and we propose to assist the population transfer with a fast-forward driving field.

The analysis of the preceding subsection can be applied to a three-state STIRAP process with  $V_0 = 0$  and the identifications

$\omega_{1,3} = 0$ ,  $\omega_{1,2}(R(t)) = \Omega_p(R(t))$ ,  $\omega_{2,3}(R(t)) = \Omega_S(R(t))$ . We choose  $R(t) = t$ , in which case  $\omega_{1,2}$  and  $\omega_{2,3}$  correspond to the Rabi frequencies of the pump and Stokes pulses. The Hamiltonian corresponding to the time-independent Schrödinger equation (2) is represented as Eq. (9). We now consider a field-dressed state

$$|\phi_2(R)\rangle = \sum_m \phi_2(m, R)|m\rangle \quad (13)$$

with  $\phi_2(1, R) = \cos \Theta(R)$ ,  $\phi_2(2, R) = 0$ ,  $\phi_2(3, R) = -\sin \Theta(R)$ , and  $\phi_2(3, R)/\phi_2(1, R) = -\Omega_p(R)/\Omega_S(R)$ . As mentioned earlier,  $m = 2$  is treated separately because  $\phi_2(2, R) = 0$ . For  $m = 2$  Eqs. (7) and (8) take the form

$$\begin{aligned} \omega_{2,1}^{\text{FF}}(t)e^{if_1}\phi_2(1, R) \\ + \omega_{2,3}^{\text{FF}}(t)e^{if_3}\phi_2(3, R) = 0, \end{aligned} \quad (14)$$

and

$$\omega_{2,1}(R)\phi_2(1, R) + \omega_{2,3}(R)\phi_2(3, R) = 0, \quad (15)$$

respectively. Combining Eqs. (14) and (15) we obtain

$$\frac{\omega_{2,1}^{\text{FF}}(t)}{\omega_{2,3}^{\text{FF}}(t)} = e^{i\Delta f} \frac{\omega_{2,1}(R(t))}{\omega_{2,3}(R(t))}, \quad (16)$$

with

$$\Delta f(t) \equiv f_3(t) - f_1(t). \quad (17)$$

Noting that  $\phi_2(2, R) = 0$  and  $\phi_2(1, R), \phi_2(3, R) \in R$ , Eq. (5) can be

rewritten as

$$\begin{aligned}\frac{dR(t)}{dt} \frac{\partial \phi_2(1, R)}{\partial R} &= \phi_2(3, R) \text{Im} \left[ \omega_{1,3}^{\text{FF}}(t) e^{i\Delta f} \right], \\ \frac{dR(t)}{dt} \frac{\partial \phi_2(3, R)}{\partial R} &= \phi_2(1, R) \text{Im} \left[ \omega_{3,1}^{\text{FF}}(t) e^{-i\Delta f} \right].\end{aligned}\quad (18)$$

It can be shown that the two equations (18) are identical by using the relations  $(\omega_{3,1}^{\text{FF}})^* = \omega_{1,3}^{\text{FF}}$  and  $\partial_R \phi_2(1, R)/\phi_2(3, R) = -\partial_R \phi_2(3, R)/\phi_2(1, R)$ , which are directly derived from  $\partial_R (|\phi_2(1, R)|^2 + |\phi_2(3, R)|^2) = 0$ . Equations (16) and (18) determine the Rabi frequencies.

We consider a fast-forwarded STIRAP process with finite  $f_m$  and vanishing diagonal elements of the driving Hamiltonian,  $V_{\text{FF}} = 0$ . Equation (6) and  $V_{\text{FF}} = 0$  lead to

$$\begin{aligned}\frac{\omega_{1,2}}{\omega_{2,3}} \text{Re}[A(t)] - \frac{df_1}{dt} &= 0, \\ \frac{\omega_{2,3}}{\omega_{1,2}} \text{Re}[A(t)] - \frac{df_3}{dt} &= 0,\end{aligned}\quad (19)$$

with

$$A(t) = \omega_{1,3}^{\text{FF}}(t) e^{i\Delta f(t)}. \quad (20)$$

$d(\Delta f)/dt$  is determined when we choose  $\text{Re}[A(t)]$  to be

$$\frac{d\Delta f(t)}{dt} = \left( \frac{1}{\tan \Theta(t)} - \tan \Theta(t) \right) \text{Re}[A(t)]. \quad (21)$$

Equation (18) determines the imaginary part of  $A$  to be

$$\text{Im}[A(t)] = \frac{d\Theta}{dt}. \quad (22)$$

Then  $\omega_{1,3}^{\text{FF}}$  is represented as

$$\begin{aligned}\omega_{1,3}^{\text{FF}} &= e^{-i\Delta f} \left( \text{Re}[A] + i \frac{d\Theta}{dt} \right) \\ &= e^{-i\Delta f} \left[ \frac{\sin 2\Theta}{2 \cos 2\Theta} \frac{d\Delta f}{dt} + i \frac{d\Theta}{dt} \right].\end{aligned}\quad (23)$$

The Rabi frequency  $\omega_{1,3}^{\text{FF}}(t)$  is complex, and must be realized by controlling the time dependences of the phases of the laser fields as well as the relative phase between  $\omega_{1,2}^{\text{FF}}$  and  $\omega_{2,3}^{\text{FF}}$ . There is an arbitrariness in the choice of  $\text{Re}[A(t)]$  or  $\Delta f(t)$ . Three different trajectories of  $A$  are depicted schematically in Fig. 1, for  $\text{Re}[A(t)] = 0$ ,  $\text{Re}[A(t)] = A_1 \exp[-t^2/\tau^2]$  and  $\text{Re}[A(t)] = A_2(t/\tau) \exp[-t^2/\tau^2]$ , with  $A_{1(2)}$  and  $\tau$  constant.

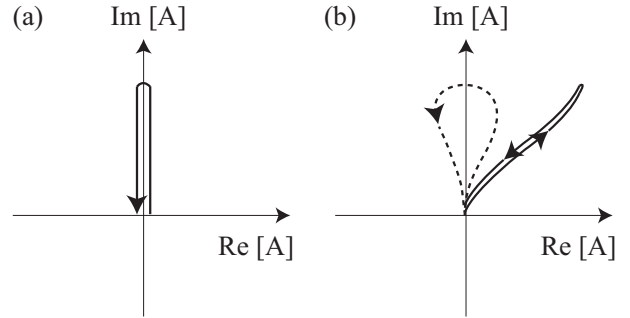


FIG. 1: Schematic diagrams of three different trajectories of  $A$ : (a)  $\text{Re}[A(t)] = 0$ ; (b)  $\text{Re}[A(t)] = A_1 \exp[-t^2/\tau^2]$  (solid curve) and  $\text{Re}[A(t)] = A_2(t/\tau) \exp[-t^2/\tau^2]$  (dotted curve) with  $A_{1(2)}$  and  $\tau$  constants.

It can be shown that the fast-forward assisted STIRAP protocol gives the same Rabi

frequencies as does the counter-diabatic field assisted STIRAP protocol with

$$f_m = 0. \quad (24)$$

Equations (16) and (23) lead to

$$\frac{\omega_{2,1}^{\text{FF}}(t)}{\omega_{2,3}^{\text{FF}}(t)} = \frac{\omega_{2,1}(R(t))}{\omega_{2,3}(R(t))}, \quad (25)$$

and

$$\omega_{1,3}^{\text{FF}} = i \frac{d\Theta}{dt}. \quad (26)$$

$\omega_{1,3}^{\text{FF}}$  in Eq. (26) is the same as the Rabi frequency of the CDF. The trajectory of  $A$  with  $\text{Re}[A(t)] = 0$  depicted in Fig. 1(a) corresponds to the CDF. Equation (25) determines the ratio of  $\omega_{2,1}^{\text{FF}}(t)$  and  $\omega_{2,3}^{\text{FF}}(t)$  but their intensities are arbitrary and can even be zero, consistent with the observation that the CDF alone can generate complete population transfer in a two-level system. When  $\text{Re}[A(t)] \neq 0$  the pulse area of the FFF pulse is larger than  $\pi$ , in contrast to the pulse area of the CDF, which is  $\pi^{14,17}$ . The restriction of the pulse area that is characteristic of the CDF protocol is eased in the fast-forward protocol.

### III. HCN→HNC ISOMERIZATION REACTION

Previous studies of STIRAP generated population transfer in laser-assisted HCN → HNC isomerization<sup>26,27</sup> have revealed that

background states coupled to the subset of states used by the driving STIRAP process degrade the population transfer efficiency. Mitigation of this inefficiency is sought in an assisted STIRAP process.

The three-dimensional potential energy surface for non-rotating HCN/HNC has been well studied<sup>28–32</sup>. The key degrees of freedom that characterize this surface are the CH, NH and CN stretching motions and the CNH bending motion. These are combined in the symmetric stretching, bending and asymmetric stretching normal modes, with quantum numbers  $(\nu_1, \nu_2, \nu_3)$ , respectively. The vibrational energy levels of HCN and HNC have been calculated by Bowman et al<sup>31</sup>. Driving the ground state-to-ground state HCN → CNH isomerization with a conventional STIRAP process that uses two monochromatic laser fields is difficult because the Franck-Condon factors between the ground vibrational states  $(0,0,0)$  of HCN and CNH and the vibrational levels close to the top of the isomerization barrier (e.g.  $(5,0,1)$ ) are extremely small. In the model system considered by Kurkal and Rice<sup>12</sup> eleven vibrational states, shown schematically in Fig. 2, are considered; rotation of the molecule is neglected. Kurkal and Rice proposed overcoming the Franck-Condon barrier with sequential STIRAP, consisting of two successive STIRAP processes. The use of this se-



quence is intended to avert the unwanted competition with other processes that can be generated by the very strong fields that would be needed to overcome the Franck-Condon barriers encountered in a single STIRAP process. In the first step of the sequential STIRAP, Kurkal and Rice chose the  $(0,0,0)$ ,  $(2,0,1)$  and  $(5,0,1)$  states of HCN as the initial, intermediate and final states, respectively; in the second STIRAP process, the  $(5,0,1)$ ,  $(2,0,1)$  and  $(0,0,0)$  states of HNC are taken as the initial, intermediate and final states, respectively. Other states, shown with dashed lines in Fig. 2, are regarded as background states. The pump 1

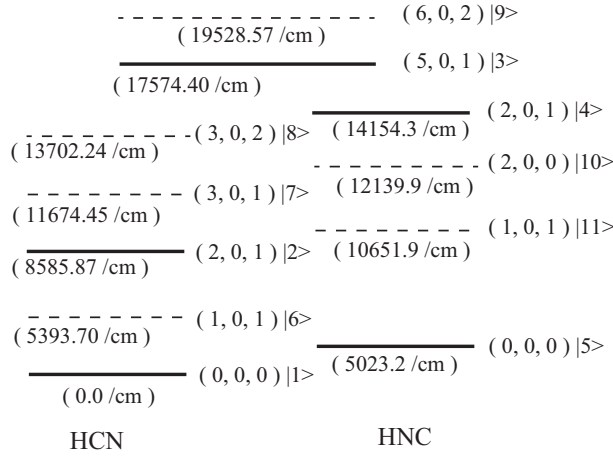


FIG. 2: Schematic diagram of the vibrational spectrum of states used for the numerical simulations. The states selected for use in the successive STIRAP processes are represented with thick lines, and the background states are represented with thin dashed lines.

field is resonant with the transition from the  $(0,0,0)$  state of HCN to the  $(2,0,1)$  state of HCN; the Stokes 1 field is resonant with the transition from the  $(2,0,1)$  state of HCN to the  $(5,0,1)$  state; the pump 2 field is resonant with the transition from the  $(5,0,1)$  state to the  $(2,0,1)$  state of HNC; and the Stokes 2 field is resonant with the transition from the  $(2,0,1)$  state to the  $(0,0,0)$  state of HNC. The transition dipole moments and the energies of the vibrational states denoted by  $|i\rangle$  are listed in Ref. 12.

Kurkal and Rice showed that the first STIRAP process is not sensitive to coupling with the background states caused by the Stokes 1 pulse<sup>12</sup>. However the second STIRAP process is influenced by interference with the background states because the intermediate state of the second STIRAP process has large transition dipole moments with the background states<sup>24</sup>. The time-dependences of the populations of states  $|1\rangle - |5\rangle$  in the sequential STIRAP process are displayed in Fig. 3. We take the strengths of the pump and the Stokes fields to be

$$E_{j,p(S)}^{(e)}(t) = \tilde{E}_{j,p(S)} \exp \left[ - \frac{(t - T_{j,p(S)})^2}{(\Delta\tau)^2} \right] \quad (27)$$

where  $\Delta\tau = \text{FWHM}/(2\sqrt{\ln 2})$ , and FWHM is the full width at half maximum of the Gaussian pulse with maximum intensity  $\tilde{E}_{j,p(S)}$  that is centered at  $T_{j,p(S)}$ , and  $j =$

(1, 2) denotes the first ( $j = 1$ ) and the second STIRAP ( $j = 2$ ) process. We solved the time-dependent Schrödinger equation numerically with a fourth order Runge-Kutta integrator in a basis of bare matter eigenstates with  $T_{j,p} - T_{j,s} = \text{FWHM}/(2\sqrt{\ln 2})$ . The parameters of the laser fields used in our calculations are shown in Table I. It is seen clearly in Fig. 3 that the fidelity of the first STIRAP in the sequential STIRAP process is robust with respect to interference from the background states<sup>24</sup>. For that reason we assume that the population is transferred from  $|1\rangle$  to  $|3\rangle$  completely, and we focus attention on the second STIRAP process, choosing  $|3\rangle$  as the initial state of the assisted STIRAP control process. States  $|1\rangle$  and  $|2\rangle$  are now and hereafter regarded as background states.

TABLE I: Strengths and widths of the pump 1, 2 and Stokes 1, 2 laser pulses.

	$\tilde{E}_{j,p(S)}$ (a.u.)	$T_{j,p(S)}$	FWHM (ps)
Stokes 1	0.00692	133	85
pump 1	0.00728	194	85
Stokes 2	0.00575	423	85
pump 2	0.00220	484	85

We now take the three vibrational states  $|3\rangle$ ,  $|4\rangle$ ,  $|5\rangle$  in Fig. 2 as the initial, intermediate and target states of both a STIRAP + FFF and a STIRAP + CDF process. We use the amplitudes and FWHMs for the pump

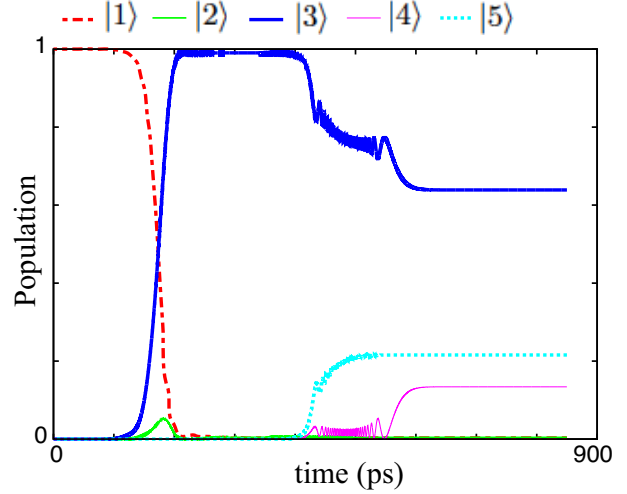


FIG. 3: Time-dependence of the several state populations for  $|1\rangle \rightarrow |5\rangle$  in the sequential STIRAP driven  $\text{HCN} \rightarrow \text{HNC}$  isomerization<sup>24</sup>.

and Stokes laser pulses listed in Table II, and choose the time-dependence of  $\text{Re}[A(t)]$  to be

$$\text{Re}[A(t)] = A_0 \exp \left[ -\frac{t^2}{\Delta\tau^2} \right] \quad (28)$$

with  $A_0 = 0.01$  /ps. The time-dependence of

TABLE II: Strengths and widths of the pump 2 and Stokes 2 laser pulses.

	$\tilde{E}_{2,p(S)}$ (a.u.)	FWHM (ps)
pump 2	0.0009295	212.5
Stokes 2	0.002875	212.5

$\Delta f$  is shown in Fig. 4(a). The phase of the Stokes field is changed by  $\Delta f$  (see Eq. (16)) and the trajectory of  $A(t) = \omega_{1,3}^{\text{FF}}(t)e^{i\Delta f(t)}$  is shown in Fig. 4(b). The amplitudes of the Rabi frequencies coupling the three states are

shown in Fig. 5(a) and the time-dependence of the population of each state in the three-state system decoupled from the background states is shown in Fig. 5(b). The data displayed clearly show that 100% population transfer is generated. As seen from Eq. (23) and Fig. 5(a) the amplitude of  $\omega_{1,3}^{\text{FF}}$  is larger than that of the CDF. The restriction of the pulse area that is characteristic of the CDF protocol is eased in the fast-forward protocol.

We now examine the efficiency of the STIRAP + FFF control when the subset of states  $|3\rangle, |4\rangle, |5\rangle$  is embedded in the manifold of states depicted in Fig. 2. We consider a FFF corresponding to Rabi frequency  $\omega_{1,3}^{\text{FF}}$  accompanied with a pump pulse and a phase-controlled Stokes field with all the background states in Fig. 2; the time-evolution of the system is calculated exactly, without use of the rotating wave approximation. In Fig. 6 the time-dependences of the populations of the initial, intermediate and the target states for (a) STIRAP and (b) STIRAP + FFF control for  $A_0 = 0.0053$  (the peak amplitude of the FFF to the CDF is about 1.2) are shown for laser pulses with FWHM = 212.5 ps and  $T_{2,p} - T_{2,S} = \text{FWHM}/(2\sqrt{\ln 2})$ . The efficiencies of both STIRAP and STIRAP + FFF controls are degraded due to interference with background states strongly coupled to the intermediate state. However

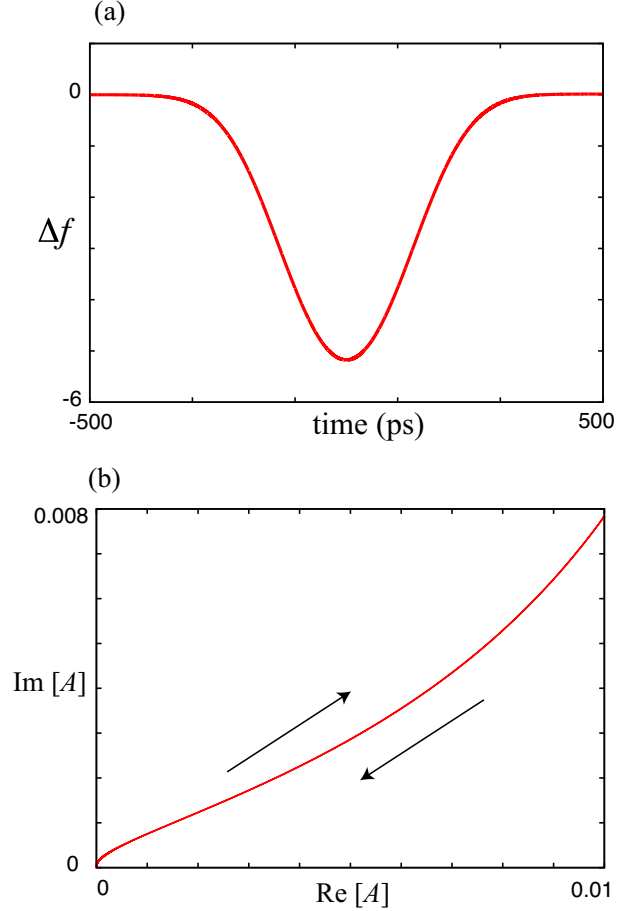


FIG. 4: The time-dependence of (a)  $\Delta f$  and (b)  $A$  for FWHM = 212.5 ps and  $T_{2,p} - T_{2,S} = \text{FWHM}/(2\sqrt{\ln 2})$ .

the influence of the background states is suppressed in the STIRAP + FFF control compared to that in the STIRAP control because of the direct coupling of the initial and target states by the FFF. Suppose now that the peak amplitude of the laser field coupling the initial and final states is larger than that of the CDF in Eq. (26) and is fixed, whilst its phase and that of the Stokes field are controllable with respect to time. As shown in

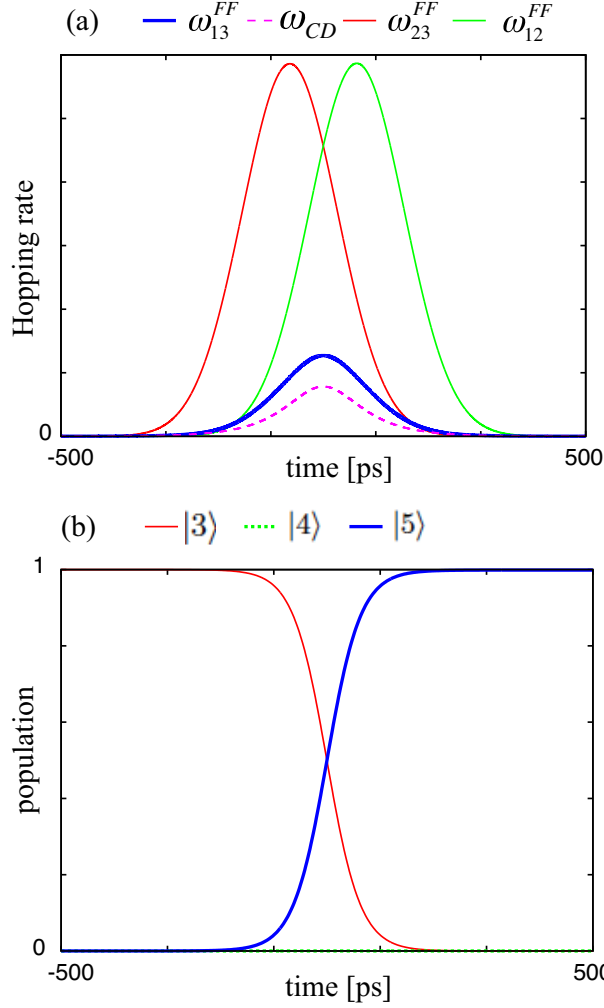


FIG. 5: (a) The time-dependences of the amplitudes of the Rabi frequencies for  $\text{FWHM} = 212.5$  ps and  $T_{2,p} - T_{2,S} = \text{FWHM}/(2\sqrt{\ln 2})$ . (b) The time-dependences of the populations.

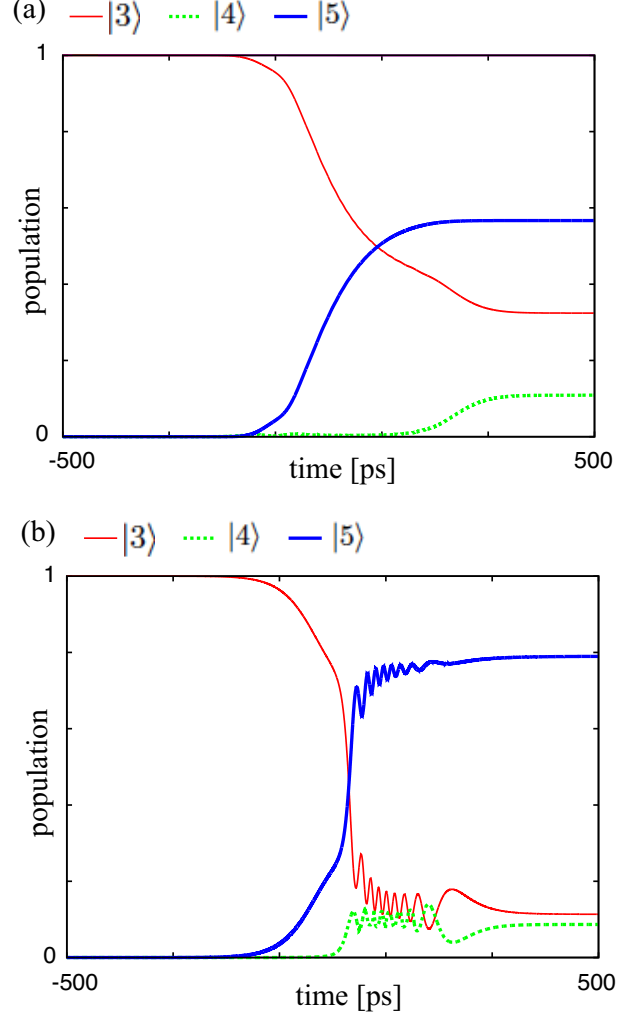


FIG. 6: Time-dependences of the populations of the initial, intermediate and the target states for (a) STIRAP and (b) STIRAP + FFF control for peak field ratio  $= 1.2$ ,  $\text{FWHM} = 212.5$  ps and  $T_{2,p} - T_{2,S} = \text{FWHM}/(2\sqrt{\ln 2})$ .

Fig. 7 the fidelity of the STIRAP + CDF control decreases when the amplitude of the laser field coupling the initial and final states is larger than that of the CDF in Eq. (26). In such cases the decrease of the fidelity is partially avoidable via phase control of the

laser fields. Five values of  $A_0$  are used; the ratio of the peak amplitude of the FFF to the CDF amplitude ranges from 1 to 1.5. In Fig. 7 we compare the calculated fidelities to that of the STIRAP + CDF control for the case

that the CDF strength is greater than that of the CDF in Eq. (26). The decrease of the fidelity due to variance of the amplitude of the CDF is reduced by phase control of the laser pulses.

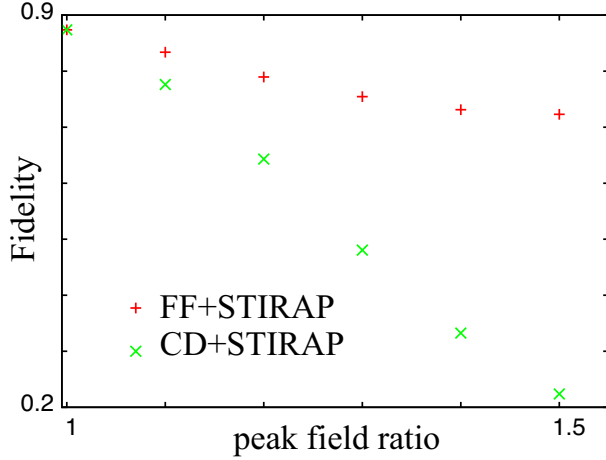


FIG. 7: The dependence of the fidelity on the peak amplitude of the laser field coupling the initial and target states. The horizontal axis is the ratio of the peak laser field amplitude to the amplitude of the CDF in Eq. (26) for FWHM = 212.5 ps and  $T_{2,p} - T_{2,s} = \text{FWHM}/(2\sqrt{\ln 2})$ .

As seen from Eq. (16), the FFF alone can generate complete population transfer to the target state in a two-level system. However the efficiency of the single pulse control is degraded when there is interaction with the background states, and is not stable to variation of the area of the pulse. So as to study the stability of the efficiency of the population transfer driven by a variable FFF we rep-

resent the total driving field in the form

$$E(t) = E_p(t) + E_S(t) + \lambda E_{\text{FF}}(t), \quad (29)$$

where  $\lambda = 0$  corresponds to driving the system with only the STIRAP fields and  $\lambda = 1$  to driving the system with the STIRAP and the FFF;  $E_{p(s)}$  is the pump (Stokes) field;  $E_{\text{FF}}$  is the FFF corresponding to the Rabi frequency in Eq. (23). In Fig. 8 the stability of the STIRAP + FFF control and the FFF alone control to the variation is monitored by the fidelity as a function of  $\lambda$ . Clearly, the sensitivity to the variation of amplitude of STIRAP + FFF control is decreased compared to that of FFF control. The STIRAP + FFF control generates higher fidelity than do STIRAP or FFF individually for a wide range of the field ratio  $\lambda$ . The value of  $\lambda$  corresponding to the peak of the fidelity of STIRAP + FFF control is smaller than one in Fig. 8, because of the interference with the background states generated by the strong fields.

The FFF, whose peak amplitude is proportional to  $1/\text{FWHM}$ , can degrade the efficiency of the control when the FWHM of the laser pulses is too short. And an increase of the field strengths in a simple STIRAP process does not generate greater population transfer efficiency because those stronger fields also generate greater interference between the active subset of states and the

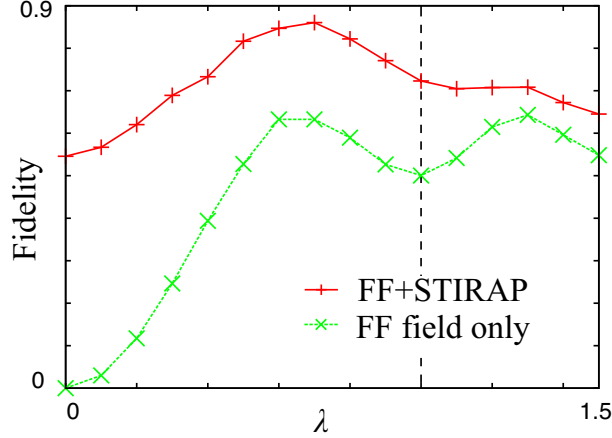


FIG. 8: Comparison of the fidelity of STIRAP+FFF control and FFF control with  $\text{FWHM} = 212.5$  ps and  $T_{2,p} - T_{2,S} = \text{FWHM}/(2\sqrt{\ln 2})$  for various  $\lambda$ .

background states<sup>24</sup>. It is seen in Fig. 9 that the FFF with  $\lambda = 0.3$  accompanied with the STIRAP fields generates higher fidelity than does the ordinary STIRAP and the STIRAP+FFFs with  $\lambda = 1$  for  $8.5 \text{ ps} \leq \text{FWHM} \leq 34 \text{ ps}$ . The drop of fidelity when FWHM decreases is due to the large intensity of the FFF. The fields associated with STIRAP and FFF generated population transfer are complementary if the amplitude of the FFF is not too large.

#### IV. VIBRATIONAL ENERGY TRANSFER IN THIOPHOSGENE

The calculations reported in Section III show that the efficiency of STIRAP+FFF generated population transfer when  $8.5 \text{ ps}$

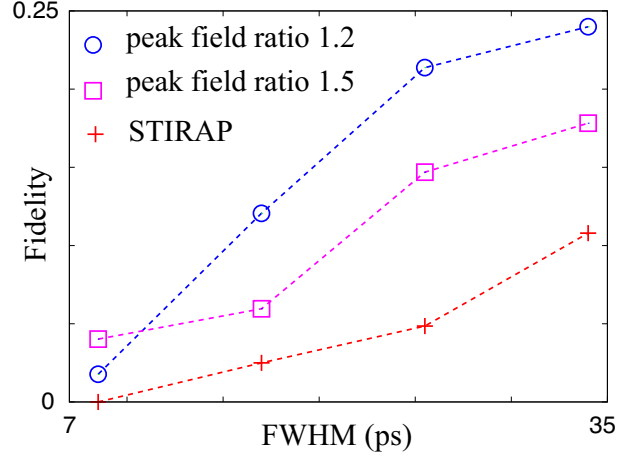


FIG. 9: FWHM-dependence of the fidelity for the STIRAP+FFF control (FF field ratio=1.2 and 1.5),  $\lambda = 0.3$  and STIRAP with  $\tilde{E}_{2,p} = 0.003718$  a.u.,  $\tilde{E}_{2,S} = 0.0115$  a.u. and  $T_{2,p} - T_{2,S} = \text{FWHM}/(2\sqrt{\ln 2})$ .

$\leq \text{FWHM} \leq 34 \text{ ps}$  is comparable to or less than that of STIRAP+CDF generated population transfer for the same pulse width range despite the extra flexibility of STIRAP+FFF compared to STIRAP + CDF contributed by phase tuning in the former. In this Section we show that that extra flexibility of STIRAP+FFF indeed can generate more efficient population transfer than STIRAP+CDF in the small FWHM regime, using as an example state-to-state vibrational energy transfer in nonrotating  $\text{SCCl}_2$ .

The  $\text{SCCl}_2$  molecule has three stretching ( $\nu_1, \nu_2, \nu_3$ ) and three bending ( $\nu_4, \nu_5, \nu_6$ ) vibrational degrees of freedom; it suffices, for our purposes, to use the same set of ener-

gies and transition dipole moments as used by Kurkal and Rice<sup>11</sup>, covering the range 0 – 21,000 cm<sup>-1</sup>, determined by Bigwood, Milam and Gruebele<sup>33</sup>. These energy levels are displayed in Fig. 10 and tabulated in Ref. 11. We will focus attention on the efficiency with which population transfer can be selectively directed to one of a pair of nearly degenerate states in the presence of background states. As in Ref. 24, we consider a STIRAP process within the subset of three states ( $|200000\rangle, |300000\rangle, |200020\rangle$ ) embedded in the full manifold of states. Hereafter we refer to these three states as  $|1\rangle$ ,  $|5^a\rangle$  and  $|6\rangle$ , respectively. The STIRAP+FFF control process is intended to generate higher population transfer from  $|200000\rangle$  to  $|200020\rangle$ . We note that  $|210011\rangle$ , hereafter called  $|9\rangle$ , with energy 5658.1828 cm<sup>-1</sup>, is nearly degenerate with  $|6\rangle$ , with energy 5651.5617 cm<sup>-1</sup>, and that the transition moment coupling states  $|1\rangle$  and  $|6\rangle$  is one order of magnitude smaller than those coupling states  $|1\rangle$  and  $|9\rangle$  and  $|5^a\rangle$  and  $|9\rangle$ .

To compare the efficiency of the STIRAP+FFF control to that of the STIRAP+CDF control we examine the dependence of the STIRAP+FFF generated population transfer on the peak ratio of the FFF to the CDF. The range of the phase tuned in the STIRAP+FFF control increases when the peak field ratio becomes large, while the

population transfer when the peak field ratio is one is identical to that generated by STIRAP+CDF without phase tuning. Figure 11 displays the dependence of the STIRAP+FFF generated population transfer on the peak ratio of the FFF to the CDF for the parameters FWHM= 21.5 ps,  $T_p - T_S = \text{FWHM}/(2\sqrt{\ln 2})$ ,  $\lambda = 1$ ,  $\tilde{E}_p = 0.014872$  a.u. and  $\tilde{E}_S = 0.046$  a.u. For a wide range of peak field ratio the population transfer generated by STIRAP+FFF exceeds that generated by STIRAP+CDF. Figure 12 displays the dependence of population transfer generated by STIRAP, STIRAP+CDF and STIRAP+FFF (with parameters  $\lambda = 1$  and peak field ratios 1.2 and 1.5) on the FWHM of the pulses. The values of  $\tilde{E}_{p,S}$  for each value of the FWHM have been adjusted so that the pulse areas of the pump and Stokes fields are the same as used for the calculations shown in Fig. 11. The STIRAP+FFF generated population transfer exceeds those generated by ordinary STIRAP and STIRAP+CDF for  $21.5 \text{ ps} \leq \text{FWHM} \leq 86 \text{ ps}$ .

## V. CONCLUDING REMARKS

We have examined the efficiency of STIRAP + FFF generated selective state-to-state population transfer in the vibrational manifolds of nonrotating SCCL<sub>2</sub> and the HCN→CNH isomerization. Neglecting the

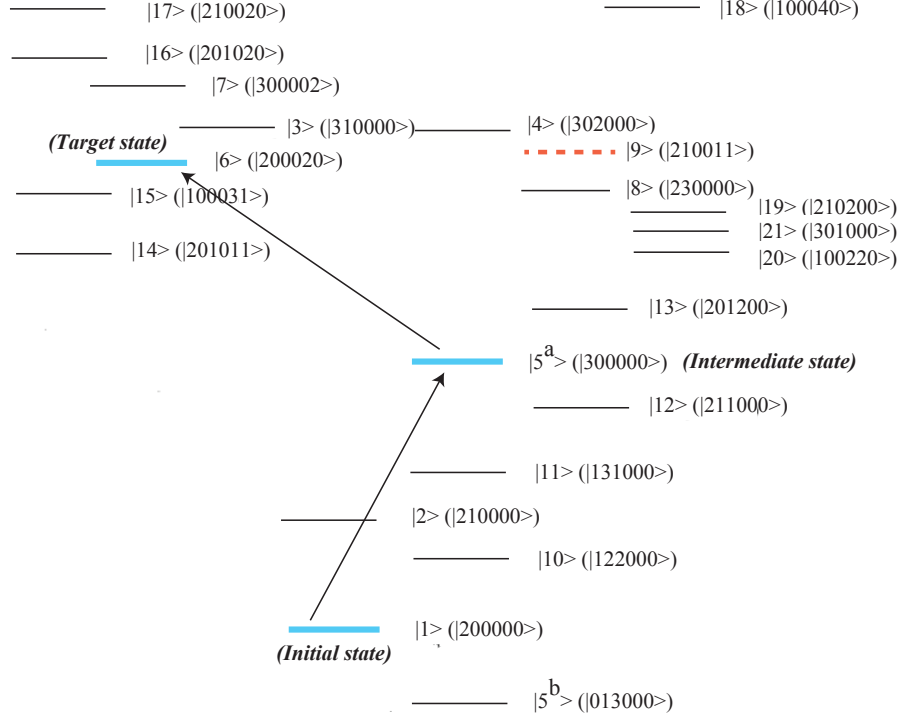


FIG. 10: Schematic diagram of the vibrational spectrum of  $\text{SCl}_2$ .

influence of molecular rotation on the efficiency of vibrational population transfer defines useful models that permit qualitative investigation of the influence of background states on the efficiency of energy transfer within an embedded subset of states, but those models are inadequate for the quantitative description of energy transfer in the corresponding real molecules. It is relevant to ask if our calculations provide a qualitatively valid picture applicable to real situations.

We have argued elsewhere<sup>24</sup> that, neglect-

ing higher order effects such as vibration rotation interaction, we expect the rotation of a molecule to affect the state-to-state process we describe in two ways. First, the transition dipole moment projection along the field axis differs with rotational state, thereby reducing the rate of excitation. Second, the rotational wave-packet created may dephase on a time scale that is comparable with the width of the exciting field, thereby changing the dynamics of the population transfer. If the ratio of the driving field duration to the period



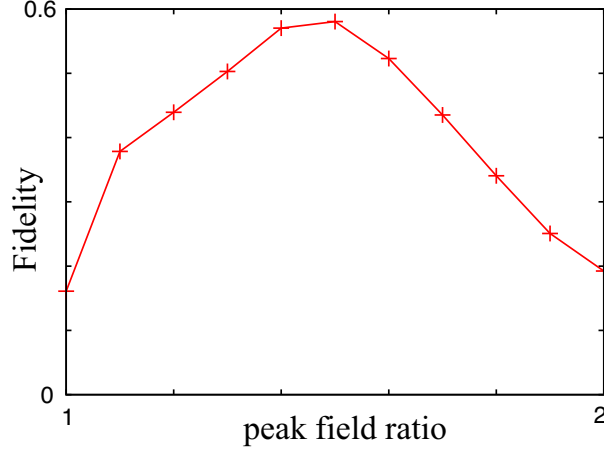


FIG. 11: The dependence of the fidelity on the peak field ratio of the FFF to the CDF for the STIRAP+FFF control with  $\text{FWHM} = 21.5$  ps,  $T_p - T_S = \text{FWHM}/(2\sqrt{\ln 2})$ ,  $\lambda = 1$ ,  $\tilde{E}_p = 0.014872$  a.u. and  $\tilde{E}_S = 0.046$  a.u.

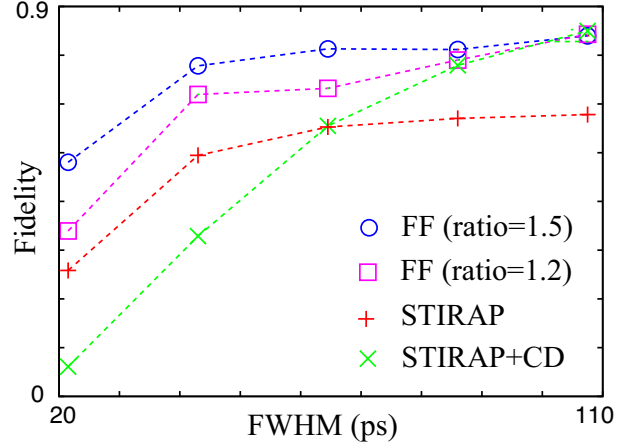


FIG. 12: The dependence of the fidelity on the FWHM for the ordinary STIRAP, the STIRAP+CDF control and the STIRAP+FFF with  $\lambda = 1$ ,  $T_p - T_S = \text{FWHM}/(2\sqrt{\ln 2})$  and the peak field ratio = 1.2 and 1.5.

of molecular rotation is very small we expect molecular rotation to have negligible influence on the population transfer, and when the period of molecular rotation is comparable to the width of the field pulses that drive the population transfer we must expect less efficient transfer than predicted for the non-rotating molecule. Indeed, noting that the combined STIRAP + FFF control process we describe involves both one and two photon transitions, and that the wave-packets of rotational states created by these two excitation processes have different dephasing rates, we expect the evolution of the state of the excited molecule to be complicated when the

period of rotation and the exciting field duration are comparable.

The rotational periods of  $\text{SCCl}_2$  and HCN are of the order of 200 ps and 10 ps, respectively. Our calculations of the efficiency of state-to-state population transfer in  $\text{SCCl}_2$  include cases when the FWHM of the pulsed fields is considerably smaller than 200 ps (see Fig. 12). The efficiency of the population transfer is smaller when the FWHM of the pulses is 20 ps than when it is 100 ps, but still usefully large. And since these pulse widths are of order one tenth of the rotational period it is plausible that similar efficiency of state-to-state population transfer can be achieved in the real molecule. Our calculations of the

efficiency of state-to-state population transfer in the HCN→CNH isomerization do not include cases when the FWHM of the pulsed fields is considerably smaller than the rotational period. In this case, as shown in Fig. 9, the use of very short pulses severely degrades the population transfer efficiency.

Returning to the model cases considered, we have shown that STIRAP + FFF generated state-to-state population transfer is more efficient than STIRAP generated state-to-state population transfer when applied to a subset of states embedded in and coupled to a larger manifold of states. Moreover, we have shown that the FFF calculated for an isolated subset of three states can be used to approximate the FFF applicable to a three state subset embedded in a large manifold of states even when some of the background states are strongly coupled to the intermediate state of the STIRAP process.

The FFF is designed to avert unwanted non-adiabatic population transfer at the end of the application of the pulsed field, and it directly couples the initial state to the target state thereby decreasing the sensitivity of the population transfer to the influence of background states. STIRAP + CDF generated population transfer exhibits this same decreased sensitivity for the same reason. However, the pulse area of the FFF is larger than  $\pi$ , in contrast to the pulse area of the CDF

for a STIRAP + CDF process in the same system, which is always  $\pi$ . And the STIRAP + FFF generated population transfer has, relative to STIRAP + CDF population transfer, an extra control parameter, namely the FFF amplitude. This parameter can be tuned to optimize the yield of population in a target state. In general, our model calculations show that, when the driven system of states is embedded in a large manifold of states, phase controlled STIRAP + FFF generates more efficient state-to-state population transfer than does STIRAP.

## ACKNOWLEDGMENTS

S.M. thanks the Grants-in-Aid for Centric Research of Japan Society for Promotion of Science and the JSPS Postdoctoral Fellowships for Research Abroad for its financial support.

## REFERENCES

- <sup>1</sup>S. A. Rice and M. Zhao, *Optical Control of Molecular Dynamics* (Wiley-Interscience, New York, 2000).
- <sup>2</sup>M. Shapiro and P. Brumer, *Principles of the Quantum Control of Molecular Processes* (Wiley-Interscience, New York, 2003).
- <sup>3</sup>U. Gaubatz, P. Rudecki, S. Schiemann and

- K. Bergmann, J. Chem. Phys. **92**, 5363 (1990).
- <sup>4</sup>G. W. Coulston, K. Bergmann, J. Chem. Phys. **96**, 3467 (1992).
- <sup>5</sup>T. Halfmann and K. Bergmann, J. Chem. Phys. **104**, 7068 (1996).
- <sup>6</sup>K. Bergmann, H. Theuer and B. W. Shore, Rev. Mod. Phys. **70**, 1003 (1998).
- <sup>7</sup>N. V. Vitanov, T. Halfmann, B. W. Shore and K. Bergmann, Annu. Rev. Phys. Chem. **52**, 763 (2001).
- <sup>8</sup>M. N. Kobrak and S. A. Rice, Phys. Rev. A **57**, 1158 (1998).
- <sup>9</sup>M. N. Kobrak and S. A. Rice, Phys. Rev. A **57**, 2885 (1998).
- <sup>10</sup>M. N. Kobrak and S. A. Rice, J. Chem. Phys. **109**, 1 (1998).
- <sup>11</sup>V. Kurkal and S. A. Rice, J. Phys. Chem. B, **105**, 6488 (2001).
- <sup>12</sup>V. Kurkal and S. A. Rice, Chem. Phys. Lett. **344**, 125 (2001).
- <sup>13</sup>B. T. Torosov and N. V. Vitanov, Phys. Rev. A **87**, 043418 (2013).
- <sup>14</sup>M. Demirplak and S. A. Rice, J. Phys. Chem. A **107**, 9937 (2003).
- <sup>15</sup>M. Demirplak and S. A. Rice, J. Phys. Chem. B **109**, 6838 (2005).
- <sup>16</sup>M. Demirplak and S. A. Rice, J. Chem. Phys. **129**, 154111 (2008).
- <sup>17</sup>X. Chen, I. Lizuain, A. Ruschhaupt, D. Guéry-Odelin and J. G. Muga, Phys. Rev. Lett. **105**, 123003 (2010).
- <sup>18</sup>J. G. Muga, X. Chen, A. Ruschhaupt, and D. Guéry-Odelin, J. Phys. B **42**, 241001 (2009).
- <sup>19</sup>S. Masuda and K. Nakamura, Phys. Rev. A **78**, 062108 (2008).
- <sup>20</sup>S. Masuda and K. Nakamura, Proc. R. Soc. A **466**, 1135 (2010).
- <sup>21</sup>S. Masuda and K. Nakamura, Phys. Rev. A **84**, 043434 (2011).
- <sup>22</sup>S. Masuda, Phys. Rev. A **86**, 063624 (2012).
- <sup>23</sup>S. Masuda and S. A. Rice, Phys. Rev. A **89**, 033621 (2014).
- <sup>24</sup>S. Masuda and S. A. Rice, arXiv:1409.0784 (2014).
- <sup>25</sup>K. Takahashi, Phys. Rev. A, **89**, 042113 (2014).
- <sup>26</sup>T. Cheng, H. Darmawan and A. Brown, Phys. Rev. A **75**, 013411 (2007).
- <sup>27</sup>W. Jakubetz, J. Chem. Phys. **137**, 224312 (2012).
- <sup>28</sup>A. M. Smith, S. L. Coy, W. Klemperer and K. K. Lehmann, J. Mol. Spectrosc. **134**, 134 (1989).
- <sup>29</sup>X. Yang, C. A. Rogaski and A. M. Wodtke, J. Opt. Soc. Am. B **7**, 1835 (1990).
- <sup>30</sup>D. M. Jonas, X. Yang and A. M. Wodtke, J. Chem. Phys. **97**, 2284 (1992).
- <sup>31</sup>J. M. Bowman, B. Gazdy, J. A. Bentley, T. J. Lee and C. E. Dateo, J. Chem. Phys. **99**, 308 (1993).
- <sup>32</sup>W. Jakubetz and B. L. Lan, Chem. Phys.

**217**, 375 (1997).

Chem. Phys. Lett. **287**, 333 (1998).

<sup>33</sup>R. Bigwood, B. Milam and M. Gruebele,